

Monte Carlo T/H Feedback with On-The-Fly Doppler Broadening for the VERA 3D HFP Assembly Benchmark Problem

Soomin Kang^a, Hyung Jin Shim^{a,*}

^aSeoul National University, 1 Gwanak-ro, Gwanak-gu, Seoul 151-744, Republic of Korea

*Corresponding author: shimhj@snu.ac.kr

1. Introduction

Monte Carlo is appropriate to provide reference solution because of its ability to deal with continuous energy cross sections and explicit geometry. In addition, Monte Carlo method is improved by developments of parallel computing remarkably so that it can be used for the whole-core transport analysis. In order to utilize Monte Carlo methods for the whole-core transport analysis, multi-physics calculation such as coupling of neutronics and thermal hydraulics (T/H) is required. McCARD [1] developed by Seoul National University has established the T/H feedback calculation algorithm which coupled neutronics calculation and T/H calculation iteratively [2] and verified by multi-group whole-core transport solutions [3]. At that time, however, Monte Carlo method could not generate Doppler broadened cross sections during the simulations so that it just utilized the pre-generated cross section libraries with fine temperature interval.

In recent years, on-the-fly Doppler broadening methods [4-8] are developed and applied to Monte Carlo codes and thus T/H feedback calculation becomes possible without significant errors of cross sections. McCARD has implemented three on-the fly Doppler broadening methods which are SIGMA1 kernel [9], Leal-Hwang Doppler broadening (LHDB) [10,11] and Gauss-Hermite quadrature (GHQ) [4].

In this study, GHQ method in McCARD is applied to 3-D hot zero power (HZZP) assembly of the CASL/VERA core physics benchmark progression problem [12]. In addition, iterative T/H feedback algorithm with GHQ method is utilized to analyze 3-D hot full power (HFP) assembly of the VERA benchmark and validated.

2. Methodology

2.1 Gauss-Hermite quadrature method

The well-known Doppler broadening equation [13] is given as

$$\sigma(v, T) = \frac{\alpha^{1/2}}{\pi^{1/2} v^2} \int_{-\infty}^{\infty} \sigma(V, T') V^2 e^{-\alpha(V-v)^2} dV \quad (1)$$

where

$$\alpha = \frac{M}{mk(T-T')} \quad (T > T'), \quad (2)$$

v and V are square roots of the neutron energy E at temperature T and T' , respectively. m and M are masses

of neutrons and target nuclei and k is the Boltzmann constant.

Eq. (1) can be rewritten as

$$\sigma(v, T) = \int_{-\infty}^{\infty} f(x) \exp(-x^2) dx, \quad (3)$$

where

$$x = \alpha^{-1/2} (V - v), \quad (4)$$

and

$$f(x) = \frac{1}{\pi^{1/2} v^2} (\alpha^{-1/2} x + v)^2 \sigma(\alpha^{-1/2} x + v, T'). \quad (5)$$

C. Dean et al. [5] apply Gauss-Hermite integration to Eq. (3) as

$$\sigma(v, T) = \int_{-\infty}^{\infty} f(x) \exp(-x^2) dx = \sum_{j=1}^N \omega_j f(x_j). \quad (6)$$

Fifteenth order Gauss-Hermite integration was used in McCARD for the accuracy and efficiency.

2.2 T/H feedback algorithm

For the T/H feedback calculation, neutronics calculation and T/H calculation should be iteratively coupled because of nonlinear relation between the neutron flux distribution and the temperature distribution. McCARD also adopted the iteration scheme for T/H feedback calculation which consists of two stages to take into account the calculation efficiency.

In the first stage, a small number of histories of the neutronics calculation is used to converge the flux and temperature roughly and a number of histories increases linearly with iterations so that flux and temperature distribution become more accurate. After each iteration of neutronics calculation, temperatures and densities are updated by T/H calculation. At this moment, on-the-fly Doppler broadening methods are used to calculate the cross section at the updated temperature. Iterations end when iteration number meet the criterion which is inputted by user or the temperature distribution is converged.

For the determination of convergence of the temperature distribution, three stopping criteria is used. The first criterion is to check the absolute value of difference between each T/H calculation is less than fixed value:

$$\max |T_i^{i+1} - T_i^i| \leq \Delta T \quad (7)$$

where l indicates region index and i indicates iteration index and the default value of ΔT is 10K. The second criterion is to consider uncertainty of the temperature updated by the T/H calculation:

$$|T_l^{i+1} - T_l^i| \leq a\sigma_{R,est} \quad (8)$$

where $\sigma_{R,est}$ is the standard deviation of the temperature and a is the confidence level. The number of regions that satisfy the criterion (17) should be larger than 95.6% of total regions. The last one utilizes chi-square test which is default option.

In the second stage, iterations of neutronics and T/H calculation are performed using maximum number of histories until the temperature profile is converged or iteration index meets maximum number of iterations of second stage.

The T/H solver of McCARD considers only simple problem including fuel pellet, gap, cladding and coolant. It is assumed that there is no coolant bypass flow which means all rods are isolated separately. Fuel rod is axially divided into several nodes and the coolant temperature of each axial node is calculated by the energy conservation. After the average temperature of coolant is calculated at each node, cladding temperature and pellet temperature are determined by conduction equations and gap temperature by the convection equation. Guide tubes and an instrument tube temperature are regarded as constant because of isolated rod assumption. Three annular regions in the fuel pellet are used to consider the temperature profile.

3. Results

3.1 VERA benchmark

The VERA core physics benchmark progression [12] consists of ten problems which contains 2-D pin and lattice geometry and 3-D assembly and core, etc. Problem 3 of VERA benchmark is for 3-D HZP fuel assembly at the beginning-of-life. The pin configuration is 17x17 Westinghouse geometry and axial geometry contains spacer grid, end plugs and core plates. For problem 3, 3.1 wt% fuel enrichment is used and inlet coolant temperature is set to 600K with 1300 ppm boron concentration. Problem 6 includes 3-D HFP assembly at the beginning-of-life and geometry is identical to problem 3.

GHQ method is applied to problem 3 and the result is compared to the reference solution provided by continuous energy (CE) KENO-VI code [12]. The T/H feedback calculation with GHQ in McCARD is performed to problem 6 which has no reference solution. Calculation results are compared to three simulation results which are calculated by MPACT/COBRA-TF [14], MCNP6 [15] and nTRACER. nTRACER [16] developed by Seoul National University is 3-D whole-core transport code based on planar MOC with axial SP3 solver and has internal T/H feedback calculation module. MCNP6 performed problem 6 using cell temperature

and coolant density calculated by MPACT/COBRA-TF results.

3.2 Validation of HZP assembly problem

For the on-the-fly Doppler broadening calculation, McCARD prepares the cross section library at 300K, 600K, 900K, 1200K and 1500K and performs Doppler broadening using the nearest temperature as an initial temperature which is lower than cell temperature.

Table 1 shows results from the HZP assembly simulation of problem 3. ENDF/B-VII.0 cross section library are used and CE KENO-VI results are taken as reference solution. McCARD row calculated the cross section using cross section libraries generated at problem temperature, 600K. GHQ row performed on-the-fly Doppler broadening calculation using 300K cross section libraries as an initial temperature. McCARD and GHQ simulations were performed using 100,000 histories per cycle with 1000 active cycle and 200 inactive cycle. Simulations were run on 80 Intel Xeon 2.66GHz processors and calculation time are shown. McCARD overestimated k_{eff} of 64 pcm than CE KENO-VI and on-the-fly Doppler broadening calculations gave the accurate results within a stochastic uncertainty. The calculation time of GHQ increased by just a factor of 2.09. Fig. 1 shows relative error of normalized radial power distribution between McCARD and CE KENO-VI results. Maximum error and RMS error were -0.19% and 0.09% respectively, and results were consistent within 95% confidence interval. Normalized axial power distribution is shown in Fig. 2.

Table 1. Results for VERA 3-D HZP Assembly

	k_{eff} (SD)	Difference (pcm)	Time (s)
Reference	1.17572 (0.000005)		-
McCARD	1.17636 (0.00006)	64	1958.5
GHQ	1.17653 (0.00006)	81	4105.0

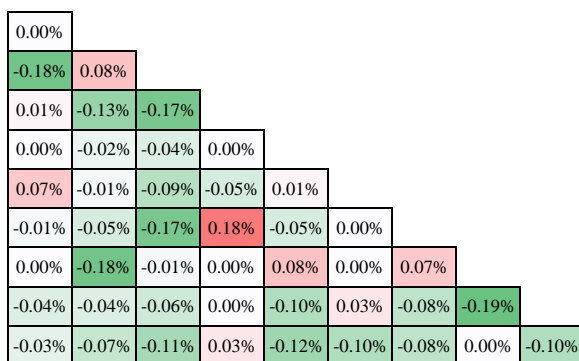


Fig. 1. Relative error of radial power distribution between CE KENO-VI and McCARD

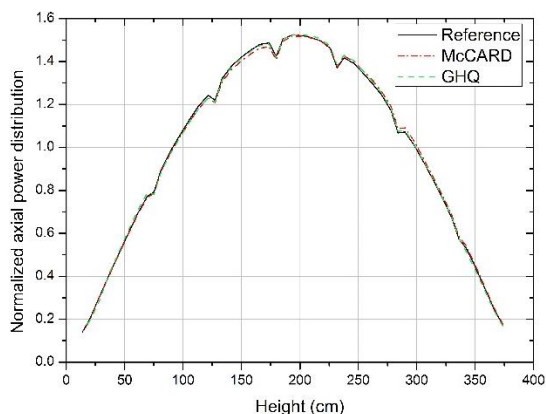


Fig. 2. Normalized axial power distribution of problem 3

3.3 Comparison of T/H feedback for HFP assembly

The geometry of 3-D HFP assembly of the problem 6 is identical to that of problem. The inlet coolant temperature is given as 565K and assembly power is 17.67 MW. Coolant flow rate of assembly is 94.4657 kg/s with 9% bypass flow. Bypass flow is ignored due to the assumption, so that flow rate is reduced by 9%. McCARD simulation was performed using ENDF/B-VII.1 libraries and 100,000 histories per cycle. The number of maximum active cycle was 1,000 and that of inactive cycle was 200. Maximum iteration of second stage was set to four to converge the temperature profile and the first stopping criterion described in section 2.2 is used to determine whether temperature profile is converged or not.

Results of each code are shown in Table 2. Since MPACT/COBRA-TF and MCNP6 used the same T/H conditions such as cell temperature and coolant density, it is obvious that results of these two codes are consistent with a difference of 33 pcm. McCARD overestimates keff of 315 pcm than MPACT/COBRA-TF and 153 pcm than nTRACER. Relative differences of radial power distribution between nTRACER and McCARD are shown in Fig. 3 which provides -0.59% maximum error with 0.25% RMS error. Normalized axial power distributions of nTRACER and McCARD are compared in Fig. 4.

The axial temperature profile of fuel pin located at next to center pin are shown in Fig. 5 where dashed lines indicate results of nTRACER and solid lines represent results of McCARD. nTRACER divided axial fuel region into two times compared to McCARD and divided annular region in the fuel pellet into five regions while McCARD divided into three regions. McCARD underestimated fuel pellet temperature compared to nTRACER above the half height. That results in overestimation of k_{eff} in McCARD.

Table 2. Results for VERA 3-D HFP Assembly

Code	Keff
MPACT/COBRA-TF	1.16467
MCNP6	1.16500
nTRACER	1.16629
McCARD	1.16782 (0.00006)

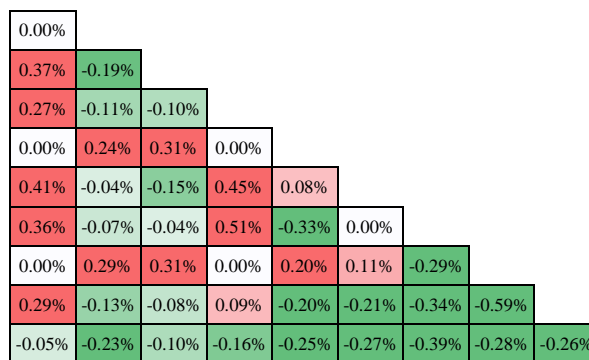


Fig. 3. Relative difference of radial power distribution between nTRACER and McCARD

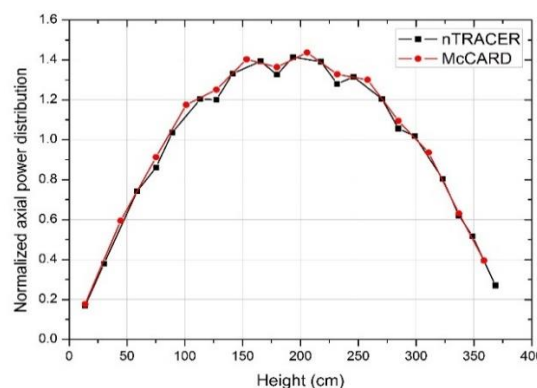


Fig. 4. Normalized axial power distribution of problem 6

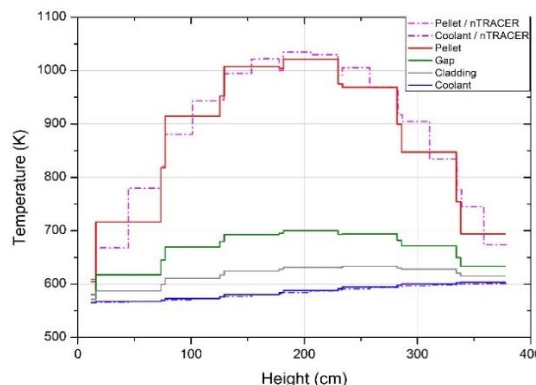


Fig. 5. Axial temperature profile located at next to center pin.

4. Conclusion

On-the-fly Doppler broadening method was applied to HZP assembly of VERA benchmark and provided

equivalent solutions within statistical errors. Normalized radial power of HZP assembly of CE KENO-VI and McCARD agreed well within 0.19%. Iterative T/H feedback algorithm with on-the-fly Doppler broadening was applied to HFP assembly and results had difference of 315 pcm compared to MPACT/COBRA-TF and 153 pcm compared to nTRACER.

Reference

1. Shim HJ, Han BS, Jung JS, Park HJ, Kim CH, "McCARD: Monte Carlo Code for Advanced Reactor Design and Analysis," *Nucl. Eng. Technol.*, **44**, 2, 161 (2012).
2. Shim HJ, Han BS, Kim CH, "Numerical Experiment on Variance Biases and Monte Carlo Neutronics Analysis with Thermal Hydraulic Feedback," International Conference on Supercomputing in Nuclear Applications, SNA (2003)
3. Joo HG, Cho JY, Kim KY, Chang MH, Han BS, Kim CH, "Consistent Comparison of Monte Carlo and Whole-Core Transport Solutions for Cores with Thermal Feedback," Proc. PHYSOR 2004, Chicago, Illinois, April 25-29, 2004, American Nuclear Society, (2004)
4. Trumbull TH, "Treatment of Nuclear Data for Transport Problems Containing Detailed Temperature Distributions," *Nucl. Technol.*, **156**, 75 (2006).
5. Dean C, Perry R, Neal R, Kyrieleis A, "Validation of Run-time Doppler Broadening in MONK with JEFF3.1," *J. Korean Phys. Soc.*, **59**, 2, 1162 (2011).
6. Yesilyurt G, Martin WR, Brown F, "On-the-Fly Doppler Broadening for Monte Carlo Codes," *Nucl. Sci. Eng.*, **171**, 239 (2012).
7. Viitanen T, Leppänen J, "Explicit Treatment of Thermal Motion in Continuous-Energy Monte Carlo Tracking Routines," *Nucl. Sci. Eng.*, **171**, 165 (2012).
8. Forget B, Xu S, Smith K, "Direct Doppler Broadening in Monte Carlo Simulations Using the Multipole Representation," *Ann. Nucl. Energy*, **64**, 78 (2014).
9. MacFarlane RE, Muir DW, "NJOY99.0 Code System for Producing Pointwise and Multigroup Neutron and Photon Cross Sections from ENDF/B Data," PSR-480/NJOY99.0, Los Alamos National Laboratory (2000).
10. Leal LC, Hwang RN, "A Finite Difference Method for Treating the Doppler Broadening of Neutron Cross Sections," *Trans. Am. Nucl. Soc.*, **55**, 340 (1987).
11. Larson NM, "Updated User's Guide for Sammy: Multilevel R-Matrix Fits to Neutron Data Using Bayes' Equations," Oak Ridge National Laboratory, pp. 131-133 (2008).
12. Godfrey AT, "VERA Core Physics Benchmark Progression Problem Specifications," CASL-U-2012-0131-004 (2014)
13. Cullen DE, Weisbin CR, "Exact Doppler Broadening of Tabulated Cross Sections," *Nucl. Sci. Eng.*, **60**, 199 (1976).
14. Kochunas B, Jabaay D, Collins B, Downar T, "Demonstration of Neutronics Coupled to Thermal-Hydraulics for a Full-Core Problem using COBRA-TF/MPACT," CASL-U-2014-0051-000, (2014)
15. Wilderman SJ, Martin WR, Brown F, "Simulation of CASL 3D HFP Fuel Assembly Benchmark Problem with On-The-Fly Doppler Broadening in MCNP6," CASL-U-2015-0152-000 (2015)
16. Jung YS, Shim CB, Lim CH, Joo HG, "Practical Numerical Reactor employing Direct Whole Core Neutron Transport and Subchannel Thermal/Hydraulic Solvers," *Ann. Nucl. Energy*, **62**, 357 (2013).